

A new biogenic, struvite-related phosphate, the ammonium-analog of hazenite, (NH₄)NaMg₂(PO₄)₂·14H₂O

HEXIONG YANG^{1,*}, LIVIA MARTINELLI^{2,3}, FLAVIA TASSO³, ANNA ROSA SPROCATI³, FLAVIA PINZARI^{2,4},
ZHENXIAN LIU⁵, ROBERT T. DOWNS¹ AND HENRY J. SUN⁶

¹Department of Geosciences, University of Arizona, 1040 E. 4th Street, Tucson, Arizona 85721, U.S.A.

²Istituto Centrale per il Restauro e la Conservazione del Patrimonio Archivistico e Librario, Rome, Italy

³Unità Tecnica Caratterizzazione, Prevenzione e Risanamento Ambientale, ENEA-CASACCIA, Rome, Via Anguillarese 301, 00123 Rome, Italy

⁴Consiglio per la Ricerca e la sperimentazione in Agricoltura Centro di ricerca per lo studio delle relazioni tra pianta e suolo,
Via della Navicella 2-4, 00184 Rome, Italy

⁵Geophysical Laboratory, Carnegie Institution of Washington, Washington, D.C. 20015, U.S.A.

⁶Desert Research Institute, 755 Flamingo Road, Las Vegas, Nevada 89119, U.S.A.

ABSTRACT

A new biogenic, struvite-related phosphate, the ammonium analog of hazenite (AAH), ideally (NH₄)NaMg₂(PO₄)₂·14H₂O, has been found in cultures containing the bacterial strain *Virgibacillus* sp. NOT1 (GenBank Accession Number: JX417495.1) isolated from an XVII Century document made of parchment. The chemical composition of AAH, determined from the combination of electron microprobe and X-ray structural analyses, is [(NH₄)_{0.78}K_{0.22}]NaMg₂(PO₄)₂·14H₂O. Single-crystal X-ray diffraction shows that AAH is orthorhombic with space group *Pmnb* and unit-cell parameters $a = 6.9661(6)$, $b = 25.236(3)$, $c = 11.292(1)$ Å, and $V = 1985.0(3)$ Å³. Compared with hazenite, the substitution of NH₄⁺ for K⁺ results in a noticeable increase of the average A-O ($A = \text{NH}_4^+ + \text{K}^+$) bond length and the unit-cell volume for AAH, as also observed for struvite vs. struvite-K. Both infrared and Raman spectra of AAH resemble those of hazenite, as well as struvite. Our study reveals that AAH forms only in cultures with Na-bearing solutions and pH below 10.0. No AAH or hazenite was found in experiments with the K-bearing solutions, suggesting the necessity of a Na-bearing solution for AAH formation.

Keywords: Ammonium phosphate, hazenite, struvite-type materials, biomineral, crystal structure, X-ray diffraction, infrared and Raman spectra

INTRODUCTION

Phosphate formation through microbial activities is one of the most common mechanisms for the biological transformation of inorganic phosphates (Gibson 1974; Kamnev et al. 1999; Desmidt et al. 2013). Among all biogenic phosphates, struvite, (NH₄)MgPO₄·6H₂O, is the most widespread in various environments, such as bat guano, decomposing foods, infection (e.g., urinary tract) stones in humans, water treatment facilities, and in a range of bacterial cultures (Sánchez-Román et al. 2007; Weil 2008; Desmidt et al. 2013 and references therein). The specific roles that microorganisms play in struvite formation are not well understood. It has been speculated that bacterial cell surfaces may serve as nucleation sites and biological activities provide a steady supply of phosphate and ammonia as the crystals grow (e.g., Ben Omar et al. 1994, 1995, 1998; Chen et al. 2010).

Several compounds are isotypic with, or structurally analogous to, struvite (Dickens and Brown 1972; Weil 2008; Yang et al. 2011). A general chemical formula for struvite-type materials can be expressed as $A^+M^{2+}(XO_4)_2 \cdot nH_2O$, where $n = 6-8$; $X = \text{P}$ or As ; $A = \text{NH}_4$, K , Rb , Cs , and Tl ; and $M = \text{Mg}$, Fe , Co , Ni , Zn , and Mn . A common structural feature of struvite-type compounds is that

all M cations are octahedrally coordinated by six H₂O molecules and no H₂O molecule is shared between $M(\text{H}_2\text{O})_6$ octahedra. The XO_4 tetrahedra and $M(\text{H}_2\text{O})_6$ octahedra are interlinked through hydrogen bonding. The struvite-type structure was once thought unable to accommodate A cations smaller than K⁺ (Banks et al. 1975). Nevertheless, Mathew et al. (1982) synthesized a Na-analog of struvite, NaMg(PO₄)·7H₂O, in which the small Na⁺ (relative to K⁺) is compensated by an additional H₂O molecule. More intriguingly, Yang and Sun (2004) and Yang et al. (2011) described the new biomineral hazenite, KNaMg₂(PO₄)₂·14H₂O, which possesses many structural features similar to those for both struvite-(K), KMg(PO₄)·6H₂O (Mathew and Schroeder 1979; Graeser et al. 2008) and synthetic NaMg(PO₄)·7H₂O (Mathew et al. 1982). Hazenite represents the first struvite-type phosphate that contains both K and Na as the A ions. In this paper, we report a new biologically formed phosphate, an ammonium analog of hazenite, ideally (NH₄)NaMg₂(PO₄)₂·14H₂O.

EXPERIMENTAL METHODS

Formation of the ammonium analog of hazenite (AAH)

The AAH crystals used in this study were formed in cultures containing the bacterial strain *Virgibacillus* sp. NOT1 (GenBank Accession Number: JX417495.1), which was isolated from an XVII Century document made of parchment and identified through 16S rDNA sequencing. The growth medium was prepared in Blood Agar Base N.2 (Oxoid, Code: CM0271) with the following components: Proteose

* E-mail: hyang@u.arizona.edu

TABLE 1. Agar media prepared for the biomineralization experiments

Run no.	Supplemented salt	Concentration	Final agar pH at 25 °C	Products identified
1	Na ₂ CO ₃	2%	9.5(3)	ammonium hazenite, struvite
2	Na ₂ CO ₃	5%	9.9(2)	ammonium hazenite
3	Na ₂ CO ₃	10%	10.0(2)	no visible crystals
4	NaCl	2%	6.9(1)	ammonium hazenite (very few)
5	NaCl	5%	6.9(4)	halite
6	NaCl	10%	6.7(3)	halite
7	KCl	5%	7.0(2)	sylvite
8	KCl	15%	6.6(1)	sylvite
9	K ₂ CO ₃	5%	9.9(5)	struvite-K
10	K ₂ CO ₃	15%	10.5(6)	kalicinite

Notes: The pH value for each run is an average of five measurements.

peptone 15.0 g/L; liver digest 2.5 g/L; yeast extract 5.0 g/L; sodium chloride 5.0 g/L; agar 12.0 g/L. The final pH was 7.4(2) at 25 °C. Four different salts at two or three different concentrations were added to the growth media (Table 1). A 10 mL aliquot of each salt-supplemented agar medium was used for the pH measurements before solidification using a glass electrode specific for high-viscosity samples (Methrom 6.0239.100 Viscotrode). The plates were then inoculated by surface streaking and incubated aerobically at 25 °C. Cultures were checked for crystal formation periodically for up to 60 days. As the growth media began to dry, elongated tabular or prismatic AAH crystals (up to 0.50 × 0.12 × 0.08 mm) appeared on or in the bacterial colonies in runs 1, 2, and 4 (Fig. 1).

Characterization of AAH crystals

The AAH crystals were first examined using a variable-pressure EVO 50 scanning electron microscope. Qualitative chemical analysis of AAH was performed with electron-dispersive spectroscopy following the procedure given by Gazulla et al. (2013), which revealed the major elements P, Mg, Na, K, and N, plus trace Ca. The presence of N in AAH was further confirmed by the infrared (IR) spectroscopy and X-ray structure determination (see below).

The quantitative analysis of the AAH chemical composition was conducted with a CAMECA SX100 electron microprobe at 10 kV and 5 nA, with a beam size of 20 μm to minimize the sample damage by the electron beam. The average composition of five analysis points is (wt%): P₂O₅ 42.2(4), MgO 23.7(3), Na₂O 9.0(1), K₂O 2.5(2), and CaO 0.16(8), with a sum of 77.5(6) wt%. Due to the high degree of hydration and the rapid deterioration of the sample during the microprobe analysis, this composition was used only for the estimation of cation ratios. By assuming two P cations per formula, the relative ratio of P:Mg:Na:K is 2.00:1.98:0.98:0.18. The actual composition of the crystal, [(NH₄)_{0.78}K_{0.22}]NaMg₂(PO₄)₂·14H₂O, was determined by the combination of the electron microprobe and X-ray structural analyses (see below), which can be idealized as (NH₄)NaMg₂(PO₄)₂·14H₂O.

The IR and Raman spectra of AAH were acquired at the U2A beamline of the National Synchrotron Light Source at Brookhaven National Laboratory. The details of experimental procedures and the optical layout of the beamline have been described by Liu et al. (2002).

Single-crystal X-ray diffraction data of AAH (from run 2) were collected at ambient temperature on a Bruker X8 APEX2 CCD X-ray diffractometer equipped with graphite-monochromatized MoK α radiation. All reflections were indexed on

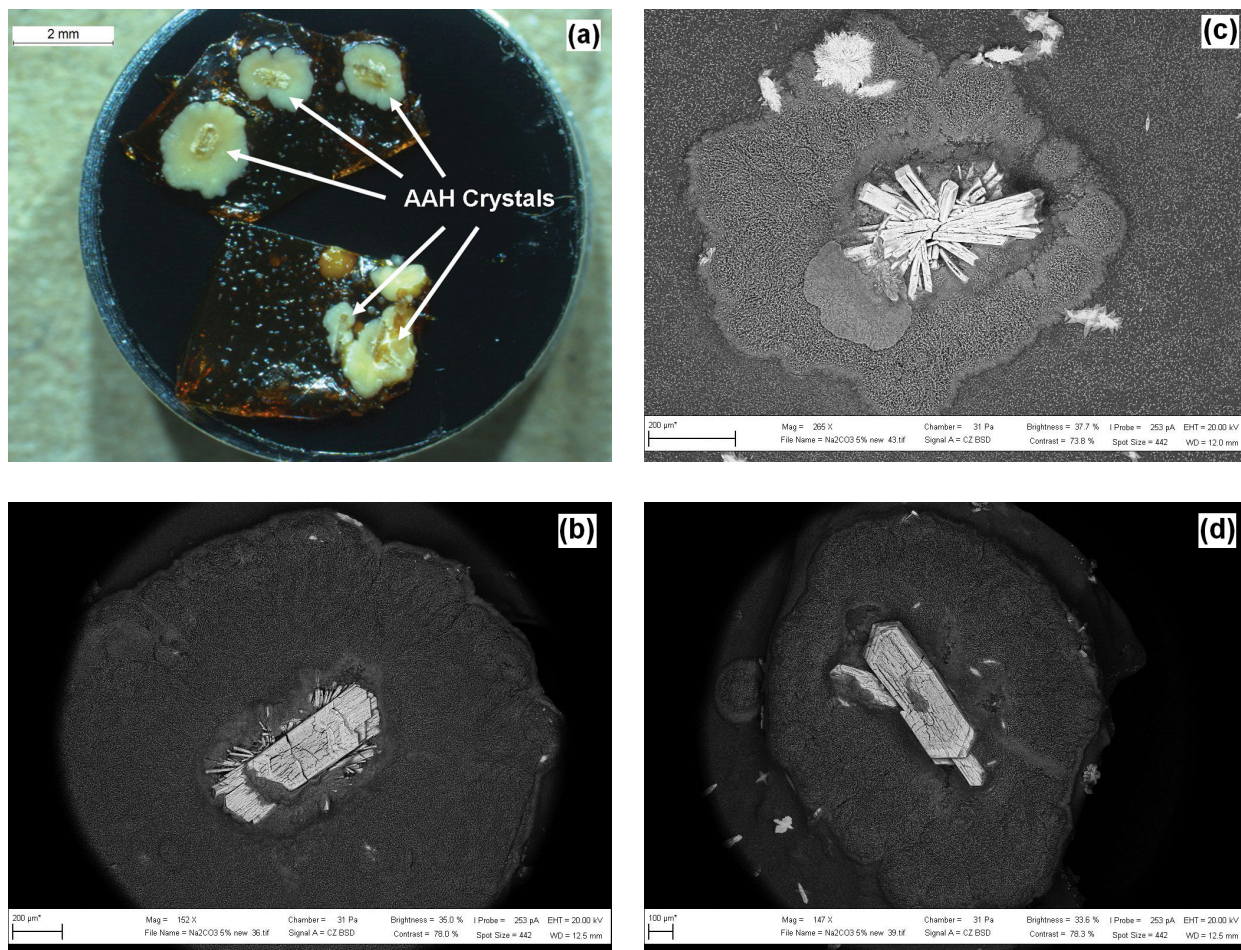


FIGURE 1. Crystals of the ammonium-analog of hazenite. (a) Crystals taken from growth run 2 (see Table 1), which are all surrounded by white bacterial colonies. Panels b, c, and d are backscattered-electron images of three colonies on the top of a (in order from left to right). (Color online.)

TABLE 2. Summary of crystallographic data and refinement results for ammonium analog of hazenite

Ideal structural formula	(NH ₄)NaMg ₂ (PO ₄) ₂ ·14H ₂ O
Space group	<i>Pmnb</i> (No. 62)
<i>a</i> (Å)	6.9661(6)
<i>b</i> (Å)	25.236(3)
<i>c</i> (Å)	11.2919(11)
<i>V</i> (Å ³)	1985.0(3)
<i>Z</i>	4
ρ_{calc} (g/cm ³)	1.795
λ (Å)	0.71069
μ (mm ⁻¹)	0.445
θ range for data collection	1.56 to 28.28
No. of reflections collected	21864
No. of independent reflections	2646
No. of reflections with $I > 2\sigma(I)$	1962
No. of parameters refined	198
R_{int}	0.068
Final <i>R</i> factors [$I > 2\sigma(I)$]	$R_1 = 0.042$, $wR_2 = 0.091$
Final <i>R</i> factors (all data)	$R_1 = 0.066$, $wR_2 = 0.099$
Goodness-of-fit	1.09

the basis of an orthorhombic unit-cell (Table 2). The intensity data were corrected for X-ray absorption using the Bruker program SADABS. The systematic absences of reflections suggest possible space group *Pmnb* (no. 62) or *P2₁nb* (no. 33). The structure model of hazenite (Yang et al. 2011) was adopted and refined using SHELX97 (Sheldrick 2008) based on the space group *Pmnb*, because it yielded the better refinement statistics in terms of bond lengths and angles, atomic displacement parameters, and *R* factors. The H atoms in all H₂O molecules were located, but not those in NH₄⁺. The positions of all atoms were refined with anisotropic displacement parameters, except for H atoms, which were refined with a fixed isotropic displacement parameter ($U_{\text{eq}} = 0.04$). The site occupancy of K was refined against N, yielding a relative ratio of 0.22(1):0.78(1). This ratio was adopted in our empirical formula for AAH. Final coordinates and displacement parameters of atoms are listed in Table 3, and selected bond-distances in Table 4. (CIF available.)

TABLE 3. Coordinates and displacement parameters of atoms for ammonium analog of hazenite

Atom	<i>x</i>	<i>y</i>	<i>z</i>	U_{10}	U_{11}	U_{22}	U_{33}	U_{23}	U_{13}	U_{12}
A	3/4	0.22146(6)	0.4983(1)	0.0386(6)	0.0505(11)	0.0295(9)	0.0356(10)	-0.0080(6)	0	0
Na	3/4	0.00057(7)	0.9266(2)	0.0367(6)	0.0280(10)	0.0420(11)	0.0401(11)	0.0115(8)	0	0
Mg1	3/4	0.95466(4)	0.6394(1)	0.0143(4)	0.0139(6)	0.0142(6)	0.0149(6)	0.0021(4)	0	0
Mg2	3/4	0.22385(4)	0.8370(1)	0.0160(4)	0.0185(6)	0.0152(6)	0.0141(6)	0.0007(4)	0	0
P1	1/4	0.12865(3)	0.7211(1)	0.0149(2)	0.0157(4)	0.0152(4)	0.0139(4)	-0.0009(3)	0	0
P2	3/4	0.12589(3)	0.2172(1)	0.0142(2)	0.0132(4)	0.0147(4)	0.0145(4)	0.0023(3)	0	0
O1	1/4	0.13574(10)	0.8572(2)	0.0215(5)	0.0230(12)	0.0289(13)	0.0127(12)	0.0019(10)	0	0
O2	1/4	0.18372(9)	0.6614(2)	0.0222(5)	0.0269(13)	0.0179(11)	0.0218(12)	0.0019(10)	0	0
O3	0.4317(2)	0.09817(6)	0.6845(1)	0.0201(4)	0.0172(8)	0.0206(8)	0.0224(9)	-0.0029(6)	0.0002(7)	0.0024(7)
O4	3/4	0.06616(9)	0.1907(2)	0.0241(6)	0.0229(13)	0.0153(12)	0.0341(14)	-0.0001(10)	0	0
O5	3/4	0.13598(10)	0.3515(2)	0.0219(5)	0.0224(12)	0.0281(13)	0.0151(12)	0.0007(10)	0	0
O6	0.9311(2)	0.15090(6)	0.1616(1)	0.0192(4)	0.0162(8)	0.0216(8)	0.0198(8)	0.0063(7)	0.0019(7)	-0.0014(7)
OW7	3/4	0.00987(12)	0.5072(3)	0.0292(7)	0.0207(14)	0.0318(16)	0.0352(16)	0.0180(12)	0	0
OW8	3/4	0.89480(13)	0.7615(3)	0.0366(8)	0.0145(13)	0.0469(18)	0.0484(19)	0.0336(14)	0	0
OW9	0.5359(3)	0.91630(8)	0.5449(2)	0.0253(4)	0.0237(10)	0.0349(11)	0.0173(9)	-0.0010(7)	0.0028(8)	-0.0107(8)
OW10	0.9586(3)	0.99535(7)	0.7373(2)	0.0233(4)	0.0203(9)	0.0194(9)	0.0302(10)	0.0001(7)	-0.0064(8)	-0.0016(8)
OW11	0.5341(3)	0.25019(8)	0.7262(2)	0.0292(4)	0.0306(10)	0.0182(9)	0.0387(11)	0.0070(9)	-0.0124(9)	0.0004(9)
OW12	0.9644(3)	0.19572(7)	0.9484(2)	0.0238(4)	0.0273(10)	0.0267(10)	0.0174(9)	0.0022(7)	0.0000(8)	0.0048(8)
OW13	3/4	0.15560(11)	0.7295(3)	0.0281(6)	0.0171(13)	0.0255(14)	0.0417(16)	-0.0129(12)	0	0
OW14	3/4	0.29694(11)	0.9275(3)	0.0376(8)	0.0681(22)	0.0171(14)	0.0276(16)	-0.0019(12)	0	0
OW15	0.0114(3)	0.05941(8)	0.9812(2)	0.0329(5)	0.0421(13)	0.0272(11)	0.0293(11)	-0.0019(8)	0.0093(10)	-0.0003(9)
H11	0.834(4)	0.026(1)	0.487(3)							
H21	0.843(4)	0.880(1)	0.789(3)							
H31	0.453(5)	0.899(1)	0.573(3)							
H32	0.546(5)	0.909(1)	0.473(3)							
H41	0.066(5)	0.976(1)	0.757(3)							
H42	0.994(4)	0.025(1)	0.727(3)							
H51	0.446(5)	0.228(1)	0.715(3)							
H52	0.512(5)	0.277(1)	0.717(3)							
H61	0.932(5)	0.182(1)	0.016(3)							
H62	0.053(5)	0.174(1)	0.918(3)							
H71	0.841(4)	0.136(1)	0.726(3)							
H81	3/4	0.317(2)	0.896(5)							
H82	3/4	0.300(2)	0.011(4)							
H91	0.053(5)	0.081(1)	0.946(3)							
H92	0.960(5)	0.076(1)	0.038(3)							

Note: $A = 0.78(\text{NH}_4) + 0.22 \text{K}$; the U_{10} parameters for all H atoms were fixed at 0.04.

DISCUSSION

Crystal structure

AAH is isostructural with hazenite, which exhibits many structural features resembling those of struvite-type materials (Yang and Sun 2004; Yang et al. 2011). The crystal structure of AAH is characterized by six distinct non-hydrogen cation sites, including two octahedral sites for Mg²⁺ (Mg1 and Mg2), two tetrahedral sites for P⁵⁺ (P1 and P2), one trigonal prismatic site for Na⁺, and one six-coordinated, very irregular site for A⁺. These cation sites form three types of layers that are stacked along the *b*-axis in a repeating sequence of ABCBABC... (Fig. 2), where layer A consists of Mg1(H₂O)₆ octahedra and NaO₆ trigonal prisms, layer B of P1O₄ and P2O₄ tetrahedra, and layer C of Mg2(H₂O)₆ octahedra and AO₆ polyhedra. These layers are linked together by hydrogen bonds, plus the A-O bonds between layers B and C (A-O5-P2). As noted by Yang et al. (2011), the struvite-type structure, which displays a layer stacking sequence of BCBCBC..., can be readily derived from the hazenite-type structure by replacing its layer A with layer C.

In general, because the effective radius of NH₄⁺ (1.48 Å) is larger than that of K⁺ (1.38 Å for six-coordination) (Shannon 1976), the substitution of NH₄⁺ for K⁺ in a crystal will result in the increase

¹ Deposit item AM-14-814, CIF. Deposit items are stored on the MSA web site and available via the *American Mineralogist* Table of Contents. Find the article in the table of contents at GSW (ammin.geoscienceworld.org) or MSA (www.minsocam.org), and then click on the deposit link.

TABLE 4. Selected non-hydrogen bond distances (Å) in hazenite and its ammonium analog

Hazenite		NH ₄ -analog of hazenite	
K-O5	2.672(3)	A-O5	2.720(3)
K-OW11 (×2)	2.980(2)	A-OW11 (×2)	3.068(2)
K-OW12 (×2)	2.908(2)	A-OW12 (×2)	2.940(2)
K-OW13	3.064(3)	A-OW13	3.095(3)
Avg.	2.919	Avg.	2.972
Na-OW10 (×2)	2.563(3)	Na-OW10 (×2)	2.589(3)
Na-OW15 (×2)	2.425(3)	Na-OW15 (×2)	2.429(2)
Na-OW15 (×2)	2.472(3)	Na-OW15 (×2)	2.478(2)
Avg.	2.487	Avg.	2.498
Mg1-OW7	2.032(3)	Mg1-OW7	2.042(3)
Mg1-OW8	2.040(3)	Mg1-OW8	2.046(3)
Mg1-OW9 (×2)	2.066(2)	Mg1-OW9 (×2)	2.074(2)
Mg1-OW10 (×2)	2.083(2)	Mg1-OW10 (×2)	2.095(2)
Avg.	2.062	Avg.	2.071
Mg2-OW11 (×2)	2.060(2)	Mg2-OW11 (×2)	2.066(2)
Mg2-OW12 (×2)	2.074(2)	Mg2-OW12 (×2)	2.077(2)
Mg2-OW13	2.093(3)	Mg2-OW13	2.107(3)
Mg2-OW14	2.109(3)	Mg2-OW14	2.109(3)
Avg.	2.078	Avg.	2.084
P1-O1	1.544(3)	P1-O1	1.548(3)
P1-O2	1.540(3)	P1-O2	1.544(3)
P1-O3 (×2)	1.530(2)	P1-O3 (×2)	1.538(2)
Avg.	1.536	Avg.	1.542
P2-O4	1.535(3)	P2-O4	1.537(3)
P2-O5	1.534(3)	P2-O5	1.538(3)
P2-O6 (×2)	1.543(2)	P2-O6 (×2)	1.544(2)
Avg.	1.539	Avg.	1.541

in both the average *A*-O bond length and the unit-cell volume, as have been observed in numerous compounds (e.g., Abu El-Fadl et al. 2006; Bogdanov et al. 2011; Shin 2011; Lim and Lee 2013). For AAH and hazenite, the average *A*-O bond lengths are 2.972 and 2.919 Å (Yang et al. 2011), respectively (Table 4), and the unit-cell volumes are 1985.0(5) and 1958.7(2) Å³ (Table 5). Similar results are also found for struvite vs. struvite-K (Table 5).

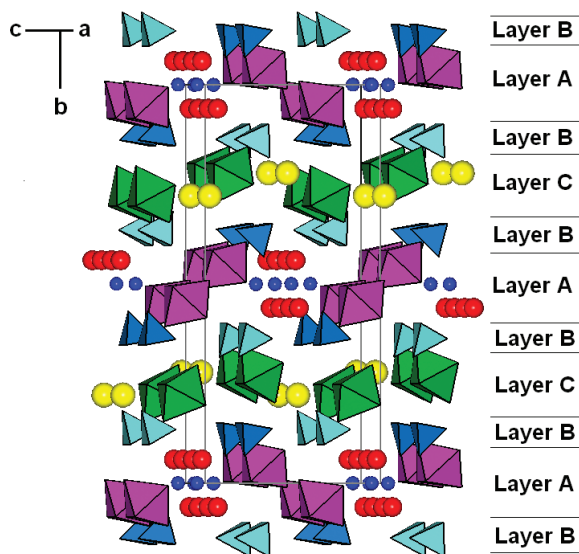


FIGURE 2. Crystal structure of the ammonium-analog of hazenite. Tetrahedra = PO₄³⁻ groups and octahedra = Mg(H₂O)₆. The largest, medium, and smallest spheres represent *A* (= NH₄+K), Ow9 (the H₂O molecule bonded to Na only), and Na, respectively. See the text for the definition of layers A, B, and C. (Color online.)

Infrared and Raman spectra

Figures 3 and 4 show the IR and Raman spectra of AAH. There have been copious IR and Raman spectroscopic studies on struvite-related materials (Banks et al. 1975; Angoni et al. 1998; Stefov et al. 2004, 2005; Frost et al. 2005; Koleva 2007; Cahil et al. 2008). Yang and Sun (2004) and Yang et al. (2011) showed that the IR and Raman spectra of hazenite are similar to those of struvite and made the tentative assignments of major bands for both spectra. These assignments should be applicable to AAH as well because of their isotypism. Nonetheless, as in the case for struvite vs. struvite-K (e.g., Stefov et al. 2005; Cahil et al. 2008), the IR spectrum of AAH is expected to be more complicated than that of hazenite owing to the presence of the significant amount of NH₄⁺. The presence of NH₄⁺ in crystals generally gives rise to two discernible groups of bands: one at ~1430 cm⁻¹ attributable to the H-N-H bending vibrations and the other at ~3300 cm⁻¹ originating from the N-H stretching vibrations, although the exact numbers and positions of bands in each group may vary, depending on the bonding environments and the local symmetry of NH₄⁺. For AAH, the bands ascribable to the H-N-H bending vibrations are observed at ~1379 and 1388 cm⁻¹. However, it is difficult to unambiguously assign which bands arise from the N-H stretching vibrations due to overlap with the O-H stretching vibrations in the range of 2700 to 3700 cm⁻¹.

Compared with the band positions for the H-N-H bending vibrations for AAH, those for struvite are at much greater wavenumbers (~1432 and 1468 cm⁻¹) (Fig. 3). This evident difference is related to the bonding environments around NH₄⁺ in the two compounds. In struvite, NH₄⁺ is coordinated by six O atoms, with a wide range of the N-O distances, from 2.800 to 3.498 Å, and an average N-O distance of 3.136 Å (Ferraris et al. 1986), whereas all six O atoms coordinated to *A* in AAH fall between 2.720 and 3.095 Å, with an average *A*-O distance of 2.972 Å (Table 4) [see Yang and Sun (2004) for a detailed discussion on the bonding differences around the *A* site between the hazenite- and struvite-type structures]. While the large separation between the two H-N-H bending modes (1468 – 1432 = 36 cm⁻¹) for struvite is primarily a consequence of the marked distortion of its *A* site, the greater wavenumbers of the two bending bands in struvite (relative to those in AAH) may be explained by its longer average N-O distance. For a N-H···O bond, the longer N-O distance means a stronger N-H and weaker H···O bonding, which makes the H-N-H bending more difficult and the corresponding bands appear at higher wavenumbers.

Implications of AAH

As shown in Table 1, AAH appears to form only in cultures with the Na-bearing solutions and pH below 10.0 (runs 1, 2, and 4). No AAH or hazenite was found in experiments with the K-bearing solutions (runs 7–10). Hence, a Na-rich environment seems to be essential for the formation of both AAH and hazenite (Yang and Sun 2004). In addition, we observed both AAH and struvite in run 1, suggesting that they are overlapping in formation environments. In nature, Mono Lake in California, which is known for its unique biological and geochemical features, currently consists of a hypersaline (84–92 g/L), alkaline (pH = 9.8) Na-CO₃-Cl-SO₄ brine (Yang et al. 2011 and references therein). This environment is obviously analogous to that of our

TABLE 5. Comparison of unit-cell data for hazenite vs. NH_4 -analog of hazenite and struvite vs. struvite-K

Name	Locality	<i>a</i> (Å)	<i>b</i> (Å)	<i>c</i> (Å)	<i>V</i> (Å ³)	References
Hazenite	Synthetic	6.9316(5)	25.1754(18)	11.2189(10)	1957.8(3)	Yang and Sun (2004)
Hazenite	Mono Lake	6.9349(4)	25.1737(15)	11.2195(8)	1958.7(2)	Yang et al. (2011)
NH_4 -hazenite	Run 1	6.962(1)	25.223(7)	11.293(2)	1983(1)	This study
NH_4 -hazenite	Run 2	6.9661(6)	25.236(3)	11.292(1)	1985.0(3)	This study
Struvite	Synthetic	6.955(1)	6.142(1)	11.218(2)	479.2(2)	Ferraris et al. (1986)
	Synthetic	6.966(1)	6.142(1)	11.217(2)	479.9(1)	Abbona et al. (1984)
Struvite	Run 1	6.956(2)	6.145(1)	11.226(4)	479.9(4)	This study
Struvite-K	Synthetic	6.873(2)	6.160(2)	11.087(3)	469.4(3)	Mathew (1979)
	Switzerland	6.892(2)	6.166(2)	11.139(4)	473.4(3)	Graeser et al. (2008)
Struvite-K	Run 9	6.8741(4)	6.1481(4)	11.1094(6)	469.51(4)	This study

experimental runs 1 or 2. Hazenite was discovered on the south shore of Mono Lake (Yang et al. 2011), where no struvite has been documented. However, on the north shore of the lake, especially on Paoha Island, where guano is relatively well preserved, struvite is quite abundant (Cooper and Dunning 1969; Walker 1988). These places, therefore, could serve as candidates for the formation and discovery of AAH in nature.

Research on the precipitation of struvite from sewage has been an attractive subject as it may offer a potential route for

dephosphorization of wastewater from industries and recovery of phosphates for fertilizers (e.g., Doyle and Parsons 2002; Shu et al. 2006; Forrest et al. 2008; Machnicha et al. 2008; Muster et al. 2013). Given the strong resemblances in both chemistry and structure between struvite and AAH, a better understanding of the formation mechanism of AAH, especially in terms of the extent of bacterial involvements, will unquestionably provide additional knowledge of biomineralization of struvite-type phosphate materials and might lead to another route for dephosphorization of wastewater. Furthermore, the struvite-type structure allows a complete substitution of AsO_4^{3-} for PO_4^{3-} (Weil 2008 and references therein). Thus, it would be intriguing to explore whether the hazenite-type structure can also have the As-analogs, synthetic or natural.

ACKNOWLEDGMENTS

This study was supported by the Science Foundation Arizona. The authors are grateful to Piero Colaizzi from the Istituto Centrale per il Restauro e la Conservazione del Patrimonio Archivistico e Librerario of Rome for his kind technical assistance with SEM-EDS. The careful and constructive reviews by U. Kolitsch and J. Pasteris are greatly appreciated.

REFERENCES CITED

- Abbona, F., Calleri, M., and Ivaldi, G. (1984) Synthetic struvite, $\text{MgNH}_4\text{PO}_4 \cdot 6\text{H}_2\text{O}$: Correct polarity and surface features of some complementary forms. *Acta Crystallographica*, B, 40, 223–227.
- Abu El-Fadl, A., Soltan, A.S., and Shaalan, N.M. (2006) Influence of cationic substitution on lattice constants and optical characterization in solution grown mixed crystals of potassium-ammonium zinc chloride. *Crystal Research and Technology*, 41, 1013–1019.
- Angoni, K., Popp, J., and Kiefe, W. (1998) A vibrational spectroscopy study of “urinary sand”. *Spectroscopy Letters*, 31, 1771–1782.
- Banks, E., Chianelli, R., and Korenstein, R. (1975) Crystal chemistry of struvite analogs of the type $\text{MgMPO}_4 \cdot 6\text{H}_2\text{O}$ ($\text{M}^+ = \text{K}^+, \text{Rb}^+, \text{Cs}^+, \text{Tl}^+, \text{NH}_4^+$). *Inorganic Chemistry*, 14, 1634–1639.
- Ben Omar, N., Entrena, M., Gonzalez-Munoz, M.T., Arias, J.M., and Huetas, F. (1994) The effects of pH and phosphate on the production of struvite by *Myxococcus Xanthus*. *Geomicrobiology Journal*, 12, 81–90.
- Ben Omar, N., Matinez-Canamero, M., Gonzalez-Munoz, M.T., Arias, J.M., and Huetas, F. (1995) *Myxococcus xanthus* killed cells as inducers of struvite crystallization: Its possible role in the biomineralization processes. *Chemosphere*, 30, 2387–2396.
- Ben Omar, N., Gonzalez-Munoz, M.T., and Penalver, J.M.A. (1998) Struvite crystallization on *Myxococcus* cells. *Chemosphere*, 36, 475–481.
- Bogdanov, E.V., Vasil’ev, A.D., Flerov, I.N., and Laptash, N.M. (2011) Effects of cation substitution in fluorine-oxygen molybdates $(\text{NH}_4)_{2-x}\text{A}_x\text{MoO}_2\text{F}_4$. *Physics of the Solid State*, 53, 303–308.
- Cahil, A., Soptrajanov, B., Najdoski, M., Lutz, H.D., Engelen, B., and Stefov, V. (2008) Infrared and Raman spectra of magnesium ammonium phosphate hexahydrate (struvite) and its isomorphous analogues. Part VI: FT-IR spectra of isomorphous isolated species. NH_4^+ ions isolated in $\text{MKPO}_4 \cdot 6\text{H}_2\text{O}$ ($\text{M} = \text{Mg}, \text{Ni}$) and PO_4^{3-} ions isolated in $\text{MgNH}_4\text{AsO}_4 \cdot 6\text{H}_2\text{O}$. *Journal of Molecular Structure*, 876, 255–259.
- Chen, L., Shen, Y., Xie, A., Huang, F., Zhang, W., and Liu, S. (2010) Seed-mediated synthesis of unusual struvite hierarchical superstructures using bacterium. *Crystal Growth and Design*, 10, 2073–2082.
- Cooper, J.F., and Dunning, G.E. (1969) Struvite found at Mono Lake. *Mineral Information Service*, 22, 44–45.

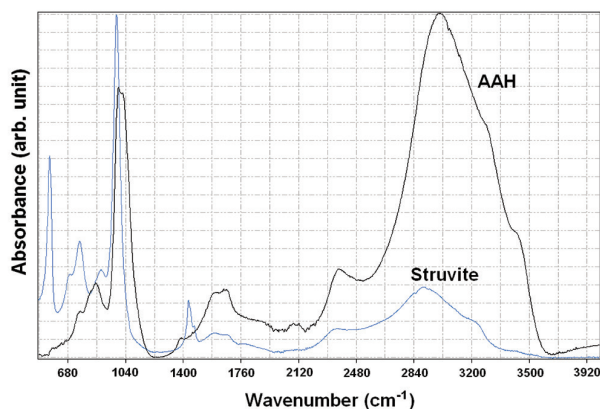


FIGURE 3. Infrared spectrum of the ammonium-analog of hazenite, along with that of struvite taken from the RRUFF project (<http://rruff.info/R050511>) for comparison. (Color online.)

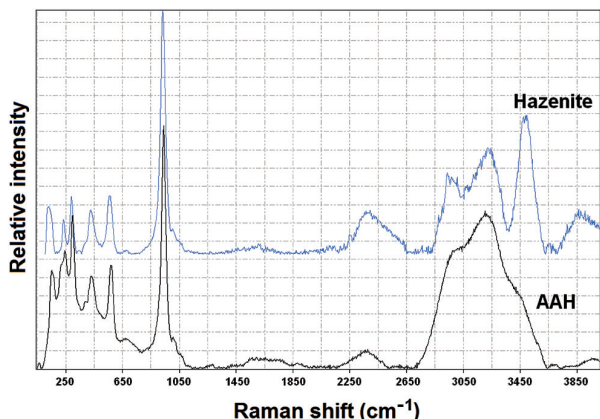


FIGURE 4. Raman spectrum of the ammonium-analog of hazenite, along with that of hazenite taken from the RRUFF project (<http://rruff.info/R100029>) for comparison. The spectra are shown with vertical offset for more clarity. (Color online.)

- Desmidt, E., Ghyselbrecht, K., Monballiu, A., Rabaey, K., Verstraete, W., and Meesschaert, B.D. (2013) Factors influencing urease driven struvite precipitation. *Separation and Purification Technology*, 110, 150–157.
- Dickens, B., and Brown, W.E. (1972) The crystal structure of $\text{CaKAsO}_4 \cdot 8\text{H}_2\text{O}$. *Acta Crystallographica*, B, 28, 3056–3065.
- Doyle, J.D., and Parsons, S.A. (2002) Struvite formation, control, and recovery. *Water Research*, 36, 3925–3940.
- Ferraris, G., Fuess, H., and Joswig, W. (1986) Neutron diffraction study of $\text{Mg}(\text{NH}_4)(\text{PO}_4) \cdot 6\text{H}_2\text{O}$ (struvite) and survey of water molecules donating short hydrogen bonds. *Acta Crystallographica*, B, 42, 253–258.
- Forrest, A.L., Fattah, K.P., Mavinic, D.S., and Koch, F.A. (2008) Optimizing struvite production for phosphate recovery in WWTP. *Journal of Environmental Engineering*, 134, 395–402.
- Frost, R.L., Weier, M.L., Martens, W.N., Henry, D.A., and Mills, S.J. (2005) Raman spectroscopy of newberyite, hannayite, and struvite. *Spectrochimica Acta*, A, 62, 181–188.
- Gazulla, M.F., Rodrigo, M., Blasco, E., and Orduna, M. (2013) Nitrogen determination by SEM-EDS and elemental analysis. *X-ray Spectrometry*, 42, 394–401, DOI:10.1002/xrs.2490.
- Gibson, R.I. (1974) Descriptive human pathological mineralogy. *American Mineralogist*, 59, 1177–1182.
- Graeser, S., Postl, W., Bojar, H.-P., Berlepsch, P., Armbruster, T., Raber, T., Ettinger, K., and Walter, F. (2008) Struvite-(K), $\text{KMgPO}_4 \cdot 6\text{H}_2\text{O}$, the potassium equivalent of struvite – a new mineral. *European Journal of Mineralogy*, 20, 629–633.
- Kamnev, A.A., Antonyuk, L.P., Colina, M., Chernyshev, A.V., and Ignatov, V. (1999) Investigation of a microbially produced structural modification of magnesium-ammonium orthophosphate. *Monatshefte für Chemie*, 130, 1431–1442.
- Koleva, V.G. (2007) Vibrational behavior of the phosphates ions in dittmarite-type compounds $M'M''\text{PO}_4 \cdot \text{H}_2\text{O}$ ($M' = \text{K}^+, \text{NH}_4^+$; $M'' = \text{Mn}^{2+}, \text{Co}^{2+}, \text{Ni}^{2+}$). *Spectrochimica Acta*, A, 66, 413–418.
- Lim, A.R., and Lee, M. (2013) Structural properties in mixed $\text{LiK}_{1-x}(\text{NH}_4)_x\text{SO}_4$ ($x = 0, 0.06$, and 1) crystals by nuclear magnetic resonance. *Journal of Molecular Structure*, 1033, 113–120.
- Liu, Z., Hu, J., Mao, H.K., and Hemley, R.J. (2002) High-pressure synchrotron X-ray diffraction and infrared microspectroscopy: Applications to dense hydrous phases. *Journal of Physics: Condensed Matter*, 14, 10641–10646.
- Machnicha, A., Grubel, K., and Suschka, J. (2008) Enhanced biological phosphorus removal and recovery. *Water Environment Research*, 80, 617–623.
- Mathew, M., and Schroeder, L.W. (1979) Crystal structure of a struvite analogue, $\text{MgKPO}_4 \cdot 6\text{H}_2\text{O}$. *Acta Crystallographica*, B, 35, 11–13.
- Mathew, M., Kingsbury, P., Takagi, S., and Brown, W.E. (1982) A new struvite-type compound, magnesium sodium phosphate heptahydrate. *Acta Crystallographica*, B, 38, 40–44.
- Muster, T.H., Douglas, G.B., Sherman, N., Seeber, A., Wright, N., and Guezuekara, Y. (2013) Towards effective phosphorus recycling from wastewater: Quantity and quality. *Chemosphere*, 91, 676–684.
- Sánchez-Román, M., Rivadeneyra, M.A., Vasconcelos, C., and McKenzie, J.A. (2007) Biomineralization of carbonate and phosphate by moderately halophilic bacteria. *FEMS Microbiology Ecology*, 61, 273–84.
- Shannon, R.D. (1976) Revised effective ionic radii and systematic studies of interatomic distances in halides and chalcogenides. *Acta Crystallographica*, A, 32, 751–767.
- Sheldrick, G.M. (2008) A short history of *SHELX*. *Acta Crystallographica*, A, 64, 112–122.
- Shin, H.K. (2011) Protonic conductivity and phase transition in $\text{K}_{1-x}(\text{NH}_4)_x\text{HSO}_4$. *Solid State Ionics*, 189, 29–32.
- Shu, L., Schneider, P., Jegatheesan, V., and Johnsom, J. (2006) An economic evaluation of phosphorus recovery as struvite from digester supernatant. *Bioresource Technology*, 97, 2211–2216.
- Stefov, V., Soptrajanov, B., Spirovski, F., Kuzmanovski, I., Lutz, H.D., and Engelen, B. (2004) Infrared and Raman spectra of magnesium ammonium phosphate hexahydrate (struvite) and its isomorphous analogues. I. Spectra of protiated and partially deuterated magnesium potassium phosphate hexahydrate. *Journal of Molecular Structure*, 689, 1–10.
- Stefov, V., Soptrajanov, B., Kuzmanovski, I., Lutz, H.D., and Engelen, B. (2005) Infrared and Raman spectra of magnesium ammonium phosphate hexahydrate (struvite) and its isomorphous analogues. III. Spectra of protiated and partially deuterated magnesium ammonium phosphate hexahydrate. *Journal of Molecular Structure*, 752, 60–67.
- Walker, J. (1988) Paoha Island phosphates. *Quarterly of San Bernardino County Museum Association*, 35, 46–47.
- Weil, M. (2008) The struvite-type compounds $M[\text{Mg}(\text{H}_2\text{O})_6](\text{XO}_4)_x$, where $M = \text{Rb}, \text{Tl}$ and $X = \text{P}, \text{As}$. *Crystal Research and Technology*, 43, 1286–1291.
- Yang, H., and Sun, H.J. (2004) Crystal structure of a new phosphate compound, $\text{Mg}_2\text{KNa}(\text{PO}_4)_2 \cdot 14\text{H}_2\text{O}$. *Journal of Solid State Chemistry*, 177, 2991–2997.
- Yang, H., Sun, H.J., and Downs, R.T. (2011) Hazenite, $\text{KNaMg}_2(\text{PO}_4)_2 \cdot 14\text{H}_2\text{O}$, a new biologically related phosphate mineral, from Mono Lake, California, U.S.A. *American Mineralogist*, 96, 675–681.

MANUSCRIPT RECEIVED OCTOBER 10, 2013

MANUSCRIPT ACCEPTED APRIL 2, 2014

MANUSCRIPT HANDLED BY FERNANDO COLOMBO